

REPORT DOCUMENTATION PAGE					<i>Form Approved</i> OMB No. 0704-0188	
The public reporting burden for this collection of information is estimated to average 1 hour per response, including the time for reviewing instructions, searching existing data sources, gathering and maintaining the data needed, and completing and reviewing the collection of information. Send comments regarding this burden estimate or any other aspect of this collection of information, including suggestions for reducing the burden, to Department of Defense, Washington Headquarters Services, Directorate for Information Operations and Reports (0704-0188), 1215 Jefferson Davis Highway, Suite 1204, Arlington, VA 22202-4302. Respondents should be aware that notwithstanding any other provision of law, no person shall be subject to any penalty for failing to comply with a collection of information if it does not display a currently valid OMB control number. PLEASE DO NOT RETURN YOUR FORM TO THE ABOVE ADDRESS.						
1. REPORT DATE (DD-MM-YYYY) 27-May-2014		2. REPORT TYPE Final			3. DATES COVERED (From - To) 05-Mar-2013 to 04-Mar-2014	
4. TITLE AND SUBTITLE UV-Assisted Reduction in BBL/Graphene Nanocomposite for Micropatterning				5a. CONTRACT NUMBER FA2386-13-1-4036		
				5b. GRANT NUMBER Grant AOARD-134036		
				5c. PROGRAM ELEMENT NUMBER 61102F		
6. AUTHOR(S) Dr. Soo-Young Park				5d. PROJECT NUMBER		
				5e. TASK NUMBER		
				5f. WORK UNIT NUMBER		
7. PERFORMING ORGANIZATION NAME(S) AND ADDRESS(ES) Kyungpook National University #1370 Sangyuk-Dong, Buk-gu Daegu 702-701 Korea (South)					8. PERFORMING ORGANIZATION REPORT NUMBER N/A	
9. SPONSORING/MONITORING AGENCY NAME(S) AND ADDRESS(ES) AOARD UNIT 45002 APO AP 96338-5002					10. SPONSOR/MONITOR'S ACRONYM(S) AFRL/AFOSR/IOA(AOARD)	
					11. SPONSOR/MONITOR'S REPORT NUMBER(S) AOARD-134036	
12. DISTRIBUTION/AVAILABILITY STATEMENT Distribution A: Approved for public release. Distribution is unlimited						
13. SUPPLEMENTARY NOTES						
14. ABSTRACT Recent extensive interest in graphene associated with its unusual properties has motivated the development of new composite materials for nanoelectronics, supercapacitors, batteries, photovoltaics, and related devices. The conjugated ladder polymer poly(benzimidazobenzophenanthroline) (BBL) has received interest as a conductive and nonlinear optical material due to its extensive π -electron delocalization, coupled with high mechanical strength, thermal stability, and good solution processability. This project involved fabrication, processing, and characterization of BBL/graphene nanocomposites and examination of film electrical properties. Composite films composed of various concentrations of BBL and graphene oxide (GO) were reduced to patterned electrically conductive films using ultraviolet light (UV). Removal the oxygen-containing functionality of the GO was confirmed by X-ray and Raman photoelectron spectroscopies, and scanning electron microscopy. Sheet resistance decreased from 10^{11} to $10^6 \Omega$ after 2 h of UV irradiation. This report provides details behind composite film processing and patterning, GO reduction, and sample characterization.						
15. SUBJECT TERMS Graphene, Nanocomposites, Micropatterning						
16. SECURITY CLASSIFICATION OF:			17. LIMITATION OF ABSTRACT	18. NUMBER OF PAGES	19a. NAME OF RESPONSIBLE PERSON Kenneth Caster, Ph.D.	
a. REPORT	b. ABSTRACT	c. THIS PAGE			19b. TELEPHONE NUMBER (Include area code) +81-42-511-2000	
U	U	U	SAR	17		

Report Documentation Page		Form Approved OMB No. 0704-0188
Public reporting burden for the collection of information is estimated to average 1 hour per response, including the time for reviewing instructions, searching existing data sources, gathering and maintaining the data needed, and completing and reviewing the collection of information. Send comments regarding this burden estimate or any other aspect of this collection of information, including suggestions for reducing this burden, to Washington Headquarters Services, Directorate for Information Operations and Reports, 1215 Jefferson Davis Highway, Suite 1204, Arlington VA 22202-4302. Respondents should be aware that notwithstanding any other provision of law, no person shall be subject to a penalty for failing to comply with a collection of information if it does not display a currently valid OMB control number.		
1. REPORT DATE 27 MAY 2014	2. REPORT TYPE Final	3. DATES COVERED 05-03-2013 to 04-03-2014
4. TITLE AND SUBTITLE UV-Assisted Reduction in BBL/Graphene Nanocomposite for Micropatterning		5a. CONTRACT NUMBER FA2386-13-1-4036
		5b. GRANT NUMBER
		5c. PROGRAM ELEMENT NUMBER 61102F
6. AUTHOR(S) Soo-Young Park		5d. PROJECT NUMBER
		5e. TASK NUMBER
		5f. WORK UNIT NUMBER
7. PERFORMING ORGANIZATION NAME(S) AND ADDRESS(ES) Kyungpook National University, #1370 Sangyuk-Dong, Buk-gu, Daegu 702-701, Korea (South), KR, 702-701		8. PERFORMING ORGANIZATION REPORT NUMBER N/A
9. SPONSORING/MONITORING AGENCY NAME(S) AND ADDRESS(ES) AOARD, UNIT 45002, APO, AP, 96338-5002		10. SPONSOR/MONITOR'S ACRONYM(S) AFRL/AFOSR/IOA(AOARD)
		11. SPONSOR/MONITOR'S REPORT NUMBER(S) AOARD-134036
12. DISTRIBUTION/AVAILABILITY STATEMENT Approved for public release; distribution unlimited		
13. SUPPLEMENTARY NOTES		
14. ABSTRACT Recent extensive interest in graphene associated with its unusual properties has motivated the development of new composite materials for nanoelectronics, supercapacitors, batteries, photovoltaics, and related devices. The conjugated ladder polymer poly(benzimidazobenzo-phenanthroline) (BBL) has received interest as a conductive and nonlinear optical material due to its extensive π-electron delocalization, coupled with high mechanical strength, thermal stability, and good solution processability. This project involved fabrication, processing, and characterization of BBL/graphene nanocomposites and examination of film electrical properties. Composite films composed of various concentrations of BBL and graphene oxide (GO) were reduced to patterned electrically conductive films using ultraviolet light (UV). Removal the oxygen-containing functionality of the GO was confirmed by X-ray and Raman photoelectron spectroscopies, and scanning electron microscopy. Sheet resistance decreased from 1011 to 106 Ω/sq; after 2 h of UV irradiation. This report provides details behind composite film processing and patterning, GO reduction, and sample characterization.		
15. SUBJECT TERMS Graphene, Nanocomposites, Micropatterning		

16. SECURITY CLASSIFICATION OF:			17. LIMITATION OF ABSTRACT Same as Report (SAR)	18. NUMBER OF PAGES 17	19a. NAME OF RESPONSIBLE PERSON
a. REPORT unclassified	b. ABSTRACT unclassified	c. THIS PAGE unclassified			

Final Report for AOARD Grant FA2386-13-1-4036 “UV-Assisted Reduction in BBL/Graphene Nanocomposite for Micropatterning”

2014-05-09

PI and Co-PI information: Soo-Young Park; psy@knu.ac.kr; Kyungpook National University; Department of Polymer Science & Engineering; 1370 Sangyeok-dong, Buk-gu, Daegu 702-701, South Korea; Phone: +82-53-950-5630; Fax: +82-53-950-6623.

Period of Performance: 03/05/2013 – 03/04/2014

Abstract: The graphene oxide (GO) film was reduced by ultraviolet (UV) irradiation which removed the oxygen-containing groups of the GO, confirmed by X-ray and Raman photoelectron spectroscopies, and scanning electron microscopy. The UV reduction of the GO film was performed at the selective areas for patterning. The sheet resistance of the GO film decreased from 10^{11} (non-conducting) to $10^6 \Omega/\square$ by UV irradiation for 2 h. The GO in the BBL/GO and PVA/GO nanocomposite films could be UV-reduced to be electrically conductive. Their sheet resistances of BBL/GO (GO content = 80 wt%) and PVA/GO (GO content = 80 wt%) films were $\sim 10^6$ and $10^5 \Omega/\square$, respectively after UV irradiation for ~ 2 h. The UV patterning of the PVA/GO film was demonstrated with “KNU” letters.

Introduction:

Graphene Properties: The recent extensive interest in graphene associated with its unique hexagonal atomic layer structure and unusual properties, including the highest intrinsic carrier mobility at room temperature of all known materials, is motivated by the development of new composite materials for nanoelectronics, supercapacitors, batteries, photovoltaics, and related devices.¹⁻⁷ Other properties of graphene such as the high thermal, chemical, and mechanical stability as well as high surface area also represent desirable characteristics as a 2-D catalyst support for metallic and bimetallic nanoparticles for a variety of applications in heterogeneous catalysis, sensors, hydrogen storage, and energy conversion.⁸⁻¹¹

Reduction of Graphene oxide: Graphite oxide (GO) is also a promising precursor for bulk production of graphene-based materials, as it can be synthesized in large quantities from inexpensive graphite powders.¹² It is usually made by reacting graphite with strong oxidants followed by gentle exfoliation.¹³ The reaction derivatizes graphene sheets with carboxylic acid, phenol hydroxyl and epoxide groups and thus breaks the π -conjugation in the two-dimensional carbon networks.¹⁴⁻¹⁵ Therefore, the resulting graphite oxide product is water dispersible, insulating, and light brown in color. The insulating GO can be reduced to form chemically modified graphene (reduced GO, rGO), in which a large portion of oxygen-containing functional groups are removed by reactions with chemical reducing agents such as hydrazine or its derivatives,¹⁶⁻²⁰ or by thermal treatment in various inert or reducing atmospheres.²¹⁻²⁴ Such deoxygenating treatments could be challenging if GO is to be blended with other materials, such as in composites. However, chemical reduction methods suffer from the difficulty of controlling the reduction process and residual contamination by the chemical reducing agents.

This can cause detrimental effects, particularly for electronic applications of graphene. Therefore, there is a need for developing deoxygenation/reduction methods that do not rely on the use of chemicals or high temperatures.

UV assisted Reduction of Graphene oxide: Reductant-free methods were developed to prepare rGO based on photodegradation. The photocatalytic reduction of the GO by TiO₂ nanoparticles was nearly completed after a few hours.²⁵⁻²⁷ But TiO₂ nanoparticles were difficult to separate from rGO nanosheets due to the interaction between TiO₂ photocatalysts and graphene. In order to meet this demand, GO has been photothermally reduced upon exposure to a pulsed Xenon flash at ambient conditions.²⁸ Using a photomask, conducting patterns such as interdigitated electrode arrays could be readily made on flexible substrates. Flash reduction was rapid, clean, and versatile and can be done with a consumer camera flash unit. It makes an insulating material conducting, enhancing its electrical conductivity by many orders of magnitude. Therefore, it could lead to many more useful applications. Compared to chemical and high temperature thermal treatments, flash reduction is rapid, chemical-free, and energy efficient. It could be an enabling technique that holds great promise for patterning GO films in device and composite applications. Femtosecond laser pulses have been used for imprinting and patterning, which resulted in partial reduction of the GO multilayer film.²⁹ Recently, a solution process was also developed for the synthesis of individual laser converted graphene (LCG) by a facile laser reduction method.³⁰ This method provided a solution processable synthesis of individual graphene sheets in water under ambient conditions without the use of any chemical reducing agent. They also reported on the high performance of GO and LCG for the efficient conversion of the laser radiation into usable heat, particularly for heating water for a variety of potential thermal, thermochemical, and thermomechanical applications.

BBL/graphene nanocomposite: Poly(benzimidazobenzophenanthroline) (BBL), a conjugated ladder polymer, has a repeat unit that possesses a double-stranded chemical structure consisting of aromatic naphthalenic and benzenoid units and alternating bond lengths of imines in the neutral ground state (Figure 1). BBL has received interest as a conductive and nonlinear optical material due to their extensive π electron delocalization, coupled with high mechanical strength and thermal stability. BBL has interesting features such as high order of thermal stability (at temperatures up to 600 °C in air and 700 °C in nitrogen), excellent chemical resistance, high electrical resistance, good solution processability, good mechanical properties as fibers and films, interesting opto-electronic properties due to its structural and molecular order, dramatically enhanced thermally induced electronic conductivity, n-type (electron transport) organic semi-conductor based on electrochemical doping experiments, photo-induced electron transfer and photoconductivity, and non-linear optical (NLO) property with large third-order optical non-linearities. These BBL properties have been evaluated for potential utilization in many opto-electronic devices that include p-n junctions, organic thin film transistors, light emitters in organic light-emitting diodes (OLEDs), tunable electrochromic and electroluminescent devices, polymer-based light sensors, xerographic imaging systems, and photovoltaic (solar) cells. Conjugated polymers such as polyacetylene, polythiophene and polyaniline have been widely studied for electronic and electro-optical properties. These polymers are insulators in pristine state and show metallic conductivity in the oxidized or reduced state. Problems encountered for practical applications of these conjugated polymers are intractability, environmental instability, and degradation upon doping. BBL belongs to a different class of conjugated polymers which are thermally and environmentally stable due to their aromatic structures. However, there are far fewer studies on the electronic transport of BBL as compared to the conventional conducting

polymers. Another aspect that has not been studied in conventional conducting polymers, primarily due to lack of thermal stability, is the behavior of electronic properties in the high-temperature ~230 to 430 °C regime at which BBL is quite stable. Pristine BBL is a semiconductor with a room temperature conductivity of 3×10^{-10} S/cm. Electrochemically doped samples show conductivities as high as 20 S/cm. Heat treatment of BBL at 100 to 350 °C dramatically and reversibly increases the room temperature dc conductivity, reaching a maximum conductivity of about 3×10^{-4} S/cm for the 350 °C treatment.

Micropatterning of the GO/Polymer composite: The use of graphene in electronic microdevices requires refined control of various complex patterns of integrated circuits³¹⁻³². Novel transfer printing methods were developed for fabricating graphene patterns by employing elastomeric stamps.³³⁻³⁴ Shadow mask was used for patterning solution-processed graphene oxide (GO) films through etching or reducing the exposed part of the GO films³⁵⁻³⁶. In addition, patterned graphene was also prepared by a successful epitaxial growth on a pre-patterned substrate.³⁷⁻³⁸ Femtosecond (FS) laser was also used to fabricate graphene microcircuits by direct reduction and patterning of GO films due to its advantages of nanometer spatial resolution and 3D prototyping capability.³⁹⁻⁴¹ Various complex patterns were successfully created through this simple FS laser nano-writing pathway. The patterned graphene was synchronously reduced and thus represent well conductivity for electrical applications. However, the UV-assisted reduction in the GO/polymer films has not fully explored for the nano-patterning. The GO/polymer composite has many advantages over the pure GO film for nanopatterning due to easy processing. The GO/polystyrene (GO/PS) composite films (prepared by filtering their mixed colloidal dispersion) have been reduced by flash reduction to make rGO/PS composites. In the GO/PS films, the polymer particles can act as a heat sink to drain away the excess heat to avoid overexposure during patterning. This helps to improve the resolution of the patterns and the integrity of the reduced domains. However, PS is a typical random coil polymer and its glass transition temperature is around 100 °C so that there is a limitation to use a patterning material in the electronic device. We have recently studied BBL/Graphene nanocomposites which were prepared through the liquid phase exfoliation of GO and rGO in methanesulfonic acid (MSA) with subsequent solution mixing.⁴² Both GO and rGO fillers were well dispersed in the BBL matrix due to π - π interactions between BBL and graphene. Compared with the pure polymer, the electrical conductivity of the nanocomposites containing 10 wt% GO and GO reduced by the combined chemical-thermal treatment showed a remarkable increase by four and seven orders of magnitude, respectively. Long-term in-situ thermal reduction was performed to further improve the conductivities of the nanocomposites. However, the BBL/GO composite has not been applied for UV-assisted reduction for micropatterning. BBL's thermal and chemical stability might be suitable for UV-assisted reduction of GO in the composite.

Purpose of this research: In this proposal, the BBL/GO dope prepared in MSA was cast into the film on the glass substrate. The well dispersed GO in BBL was reduced by UV irradiation. The conversion from GO to graphene was monitored to find a potential application for micro-patterning in device. The PVA/GO nanocomposite was also examined for UV reduction to compare it with the BBL/GO nanocomposite.

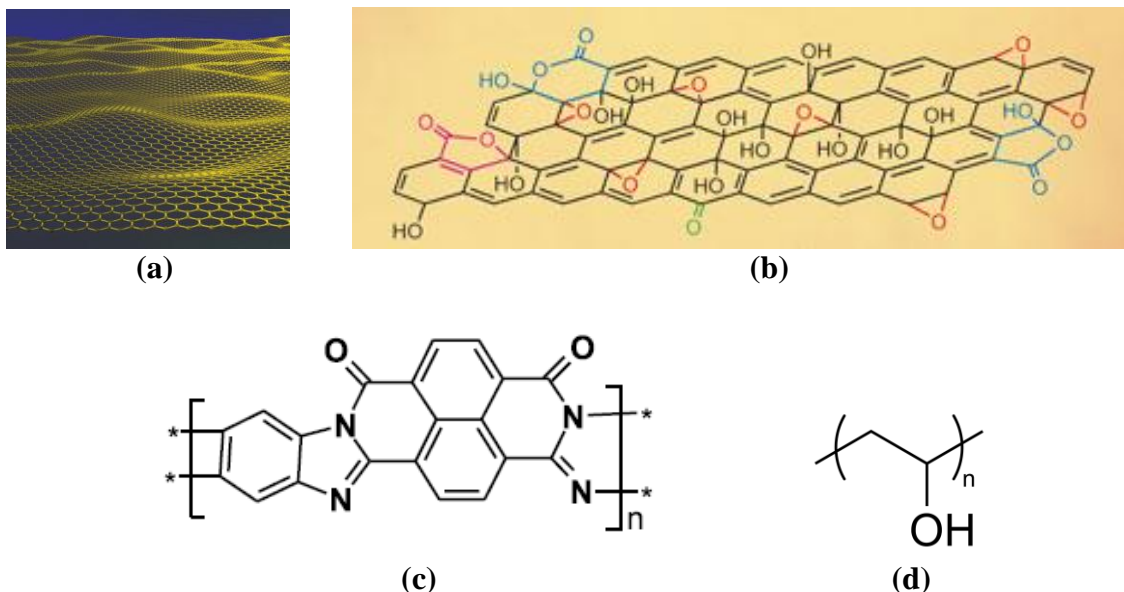


Figure 1. Chemical structures of (a) graphene, (b) graphene oxide, (c) BBL, and (d) poly(vinyl alcohol).

Experiment:

Materials: BBL(Aldrich, $M_w = 10113 \text{ g/mole}$), MSA (Alfa Aesar, 98+%), graphite (Samjung, 25 μm size), and PVA(Yakuri pure chemicals co., Japan, $M_n=1500 \text{ g/mol}$) were used as-received.

Preparation of GO: GO was synthesized by a modified Hummers method as shown in Figure 2. Briefly, 4 g graphite is added to a 500 ml flask with 92 ml concentrated H_2SO_4 and 2 g NaNO_3 . After stirring for 30 min at $< 3^\circ\text{C}$, 12 g KMnO_4 is added slowly and the reaction continues for 3 h before being terminated by the addition of 200 ml water. 30% H_2O_2 is then added to reduce the excess un-reacted KMnO_4 . The mixture is filtered with a membrane filter (50 mm diameter, 0.2 μm pore size) and washed with dilute HCl and distilled water. The resulting GO is then dried at 60°C for two days.

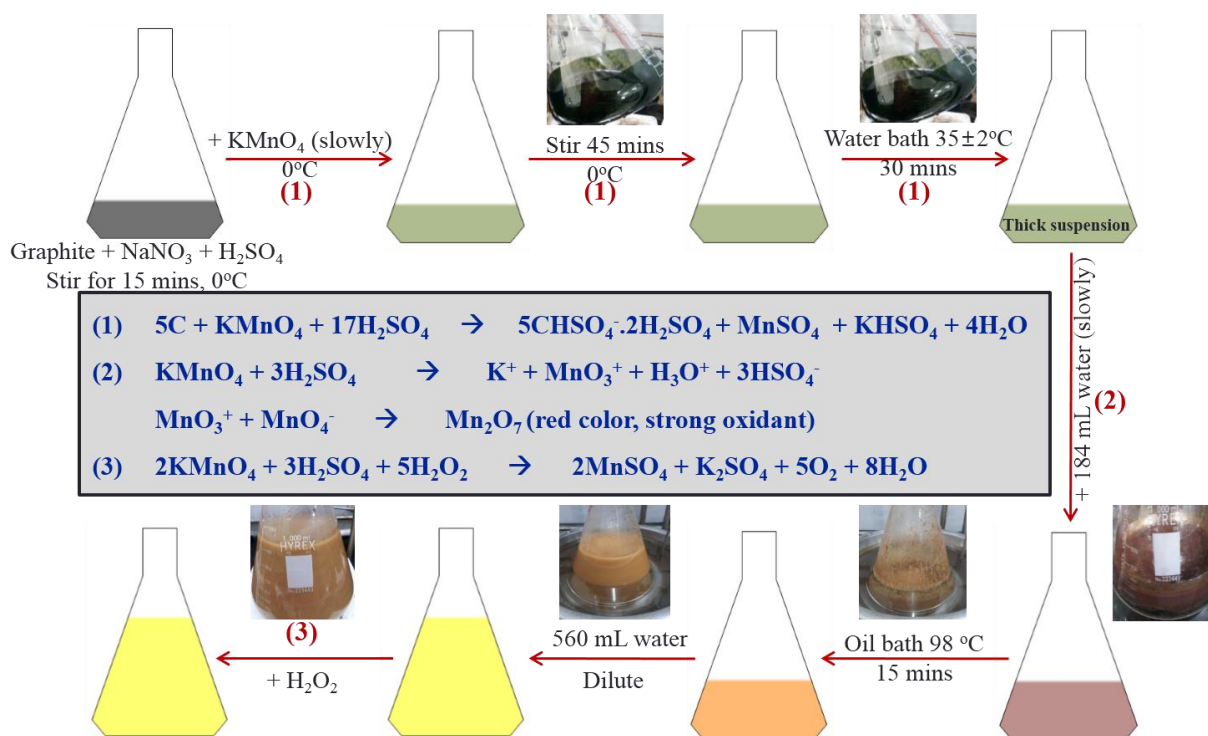


Figure 2. Schematic of GO preparation.

Preparation of GO film: The GO film was prepared by a filtration method. The GO powders (200 mg) in water (100 mL) were sonicated to make a GO aqueous solution. The solution was filtered with cellulose membrane (Advantec®, Japan, mixed cellulose ester, pore size 0.2 μm). The filtered film was 20 μm thick.

Preparation of GO/BBL film: Figure 3 shows the experimental scheme for preparing the BBL/GO thin film on the glass substrate. The GO was dispersed in methansulfonic acid (MSA, good dispersion solvent) by sonication and mixed with BBL with mixing ratios in Table 1. The amounts of GO in the composite was denoted as φ wt%

Table 1. Mixing ratio of BBL/GO solution in MSA

GO contents (φ wt%)	0	90	80	70	60	50
BBL(mg)	15	5	10	15	16	20
GO(mg)	-	45	40	35	24	20
MSA(ml)	3	2.5	2.5	2.5	2	2

The mixed BBL/GO solution was spin-cast (800 rpm) into the thin film on the glass substrate (22 × 22 mm², Duran Company, Germany) which was previously treated with O₂ plasma. MSA was removed from the thin film by washing with a mixture non-solvent of ethylalcohol/triethylamine (9/1, v/v) and drying in a vacuum oven. Spin-casting was not possible only for 90 wt% of GO in BBL/GO nanocomposites due to small amounts of matrix BBL in the nanocomposite. Preparation of the thin film of the BBL/GO film on the substrate is important to realize the application of the composite into the device. Figure 3 shows the picture

of the BBL/GO (10 wt%) spin-coated on the slide glass. The pink colored film was obtained after spin coating. This film was changed into the gold-colored film after washing with a ethanol(9)/triethylamine(1) solvent and drying.

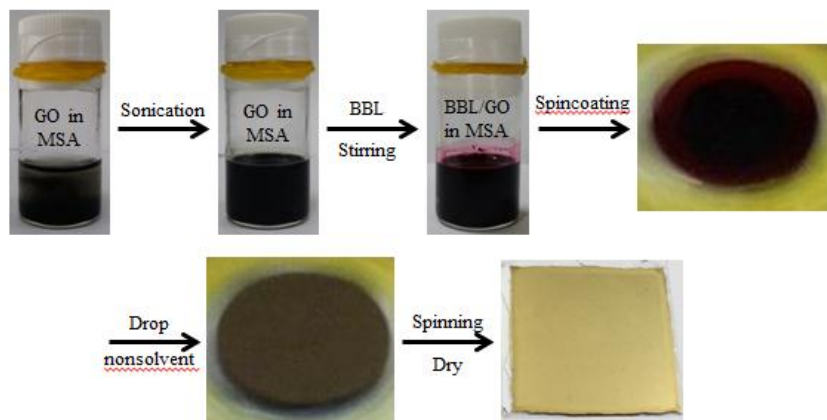


Figure 3. Sample preparation of spin-coated BBL/GO nanocomposites.

UV reduction: UV reduction was performed on the spin-coated glass at the sample to UV source distance of 5 cm which gave a UV intensity of 25 mW/cm² with a UV lamp (Lichtzen Co, spot-uv (inno cure-100N, Korea) at 365 nm.

Preparation of PVA/GO film: To test the effect of the rigidity of polymer matrix backbone on the UV reduction, the flexible polymer PVA/GO nanocomposite was prepared and compared with the BBL/GO nanocomposite. PVA is a water-soluble polymer so that GO was well dispersed in a PVA aqueous solution. GO in a vial containing water was sonicated to get a dispersed GO aqueous solution. PVA in another vial containing water was heated at 90 °C to get a clear PVA aqueous solution. The PVA aqueous solution was dropped drop-wise into the GO aqueous solution to get the PVA/GO aqueous solution. The PVA/GO aqueous solutions were poured into Teflon-taped petri dishes and dried in an oven at 60 °C for 24 h. The prepared films were 110 μm thick.

Characterization:

XPS: X-ray photoelectron spectroscopy (XPS, ULVAC-PHI, Quantera SXM, Japan) was been performed with the GO and UV-reduced GO samples using a Al K α X-ray source (1486.6 eV) in the range 0-800 eV.

SEM: Scanning electron microscopy (SEM, Hitachi, S-4800, Japan) was performed with the platinum-coated fractured surfaces in liquid nitrogen at 5 kV.

Electrical conductivity: Sheet resistance (and electrical conductivity) was with a 1 mm wide-spacing four-point probe operating by a Keithley electrometer (model 2400, USA).

Raman spectroscopy: Raman spectroscopy at 600-4000 cm⁻¹ was performed using backscattering geometry and a Raman spectrometer (Ntegra spectra NT-MDT, Russia) with excitation at 532 nm using an argon laser.

Results and Discussion:
UV reduction of the GO film:

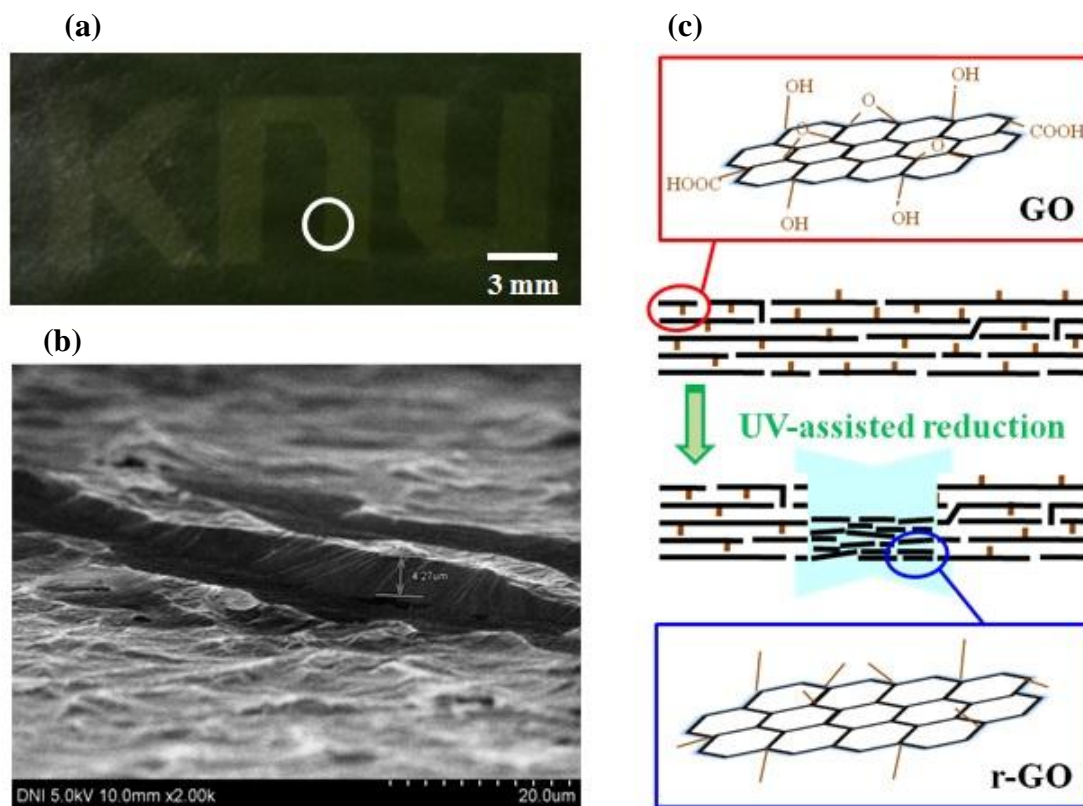


Figure 4. (a) Photo image of the GO film masked with letters of “KNU” after UV irradiation, (b) SEM image of the boundary between UV exposed and masked parts at the circled region in (a), and (c) the schematic drawing of the UV reduction of the GO film.

Figure 4 shows the photo image of the GO film masked with letters of “KNU” after UV irradiation and the SEM image at the boundary between UV exposed and masked parts. The surface of the UV exposed part was sink by $\sim 4 \mu\text{m}$ due to the removal of the oxygen containing groups in GO indicating that the reduction of the GO film happened at open region of the mask by UV beam. The boundary between UV exposed and masked parts was sharp so that the patterning of the GO film was possible from the GO film. The right part was schematic of the UV patterning of the GO film showing the sink of the UV exposed region by reduction through removal of the oxygen containing groups. Thus, we found that selective reduction of the GO film using UV irradiation through a mask was possible.

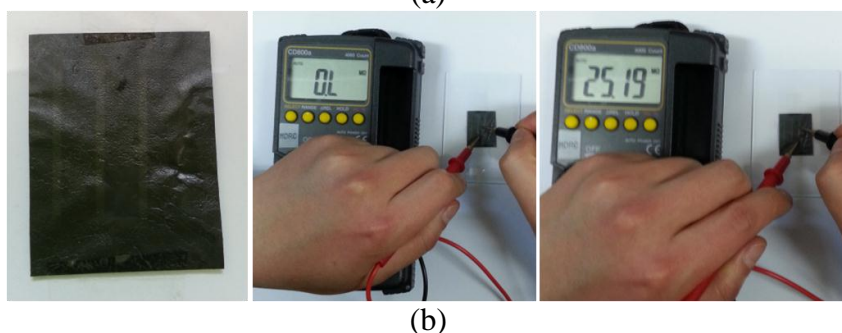
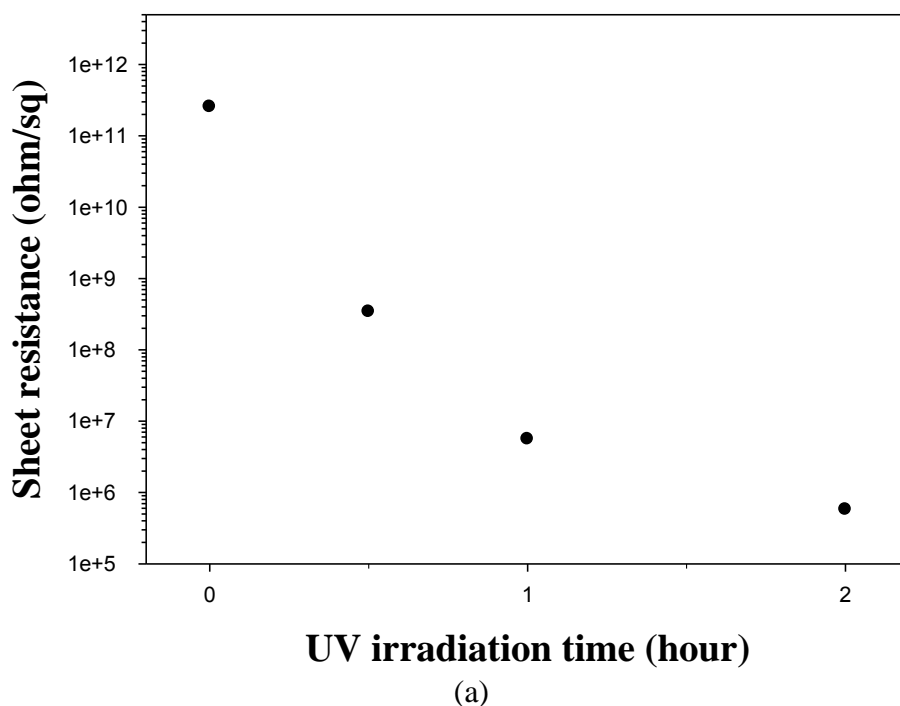


Figure 5. (a) Sheet resistance of the GO film as a function of UV irradiation time, and (b) the photo image of the GO film patterned with a line mask by UV irradiation.

Figure 5a shows the sheet resistance of the GO film as a function of UV irradiation time. The sheet resistivity continuously decreased as UV irradiation time increased. The initial $3 \times 10^{11} \Omega/\square$ before UV irradiation decreased until $6 \times 10^{11} \Omega/\square$ after 2 hour UV irradiation. Figure 5b shows the photo image of the GO film patterned with a line mask by UV irradiation. The test meter shows conductivity at the open region in the mask and non-conductivity at the close region in the mask. Thus, it clearly shows the patterning ability of the GO film. The transformations from graphite to GO and then to rGO were evaluated by Raman spectroscopy.

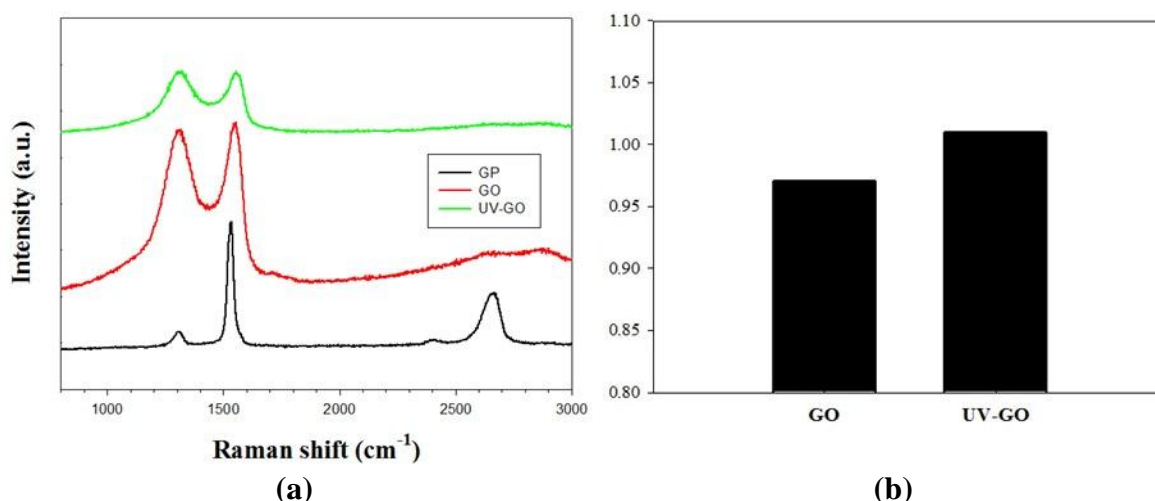
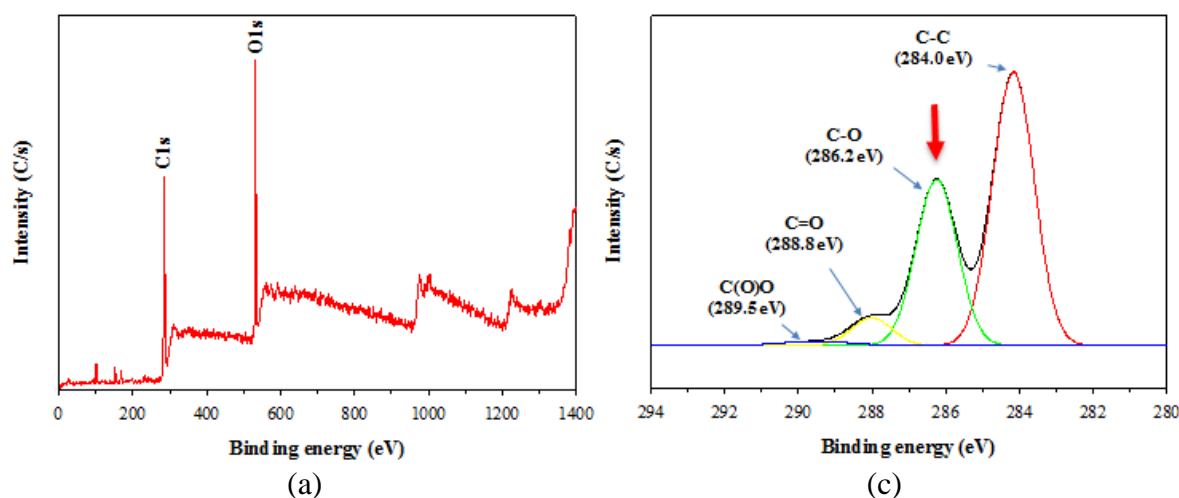


Figure 6. (a) Raman spectra of the graphite powder, the GO and the UV-irradiated GO, and (b) the I_D/I_G ratios of the GO and the UV-reduced GO.

Figure 6a shows the Raman spectra of the graphite powder, the GO and the UV-irradiated GO. The Raman spectrum of pristine graphite demonstrates a sharp G band at 1580 cm⁻¹ and a very weak D band at 1354 cm⁻¹, attributable to the first order scattering of the E_{2g} vibration mode in the graphite sheets and structural defects, respectively. In the Raman spectrum of GO, the appearance of a prominent D band at 1352 cm⁻¹ is due to the disordered structure of the graphene oxide sheets, caused by surface oxygen functional groups generated during the oxidation. The G band of the GO is broadened and blue shifted to 1597 cm⁻¹, indicating the destruction of symmetry, possibly due to the significant shrinking of the in-plane sp^2 domains caused by the extensive oxidation.^{40, 41} The significant increase in the intensity ratio of the D band to the G band (I_D/I_G) in GO compared with pristine graphite also indicates shrinking of the in-plane sp^2 domains. The UV-reduced GO sample showed higher band intensity ratios (I_D/I_G) than GO (Figure 6b), indicating an increase of sp^2 carbon in rGO and a decrease in the oxidized molecular defects upon reduction of the exfoliated GO.⁴²



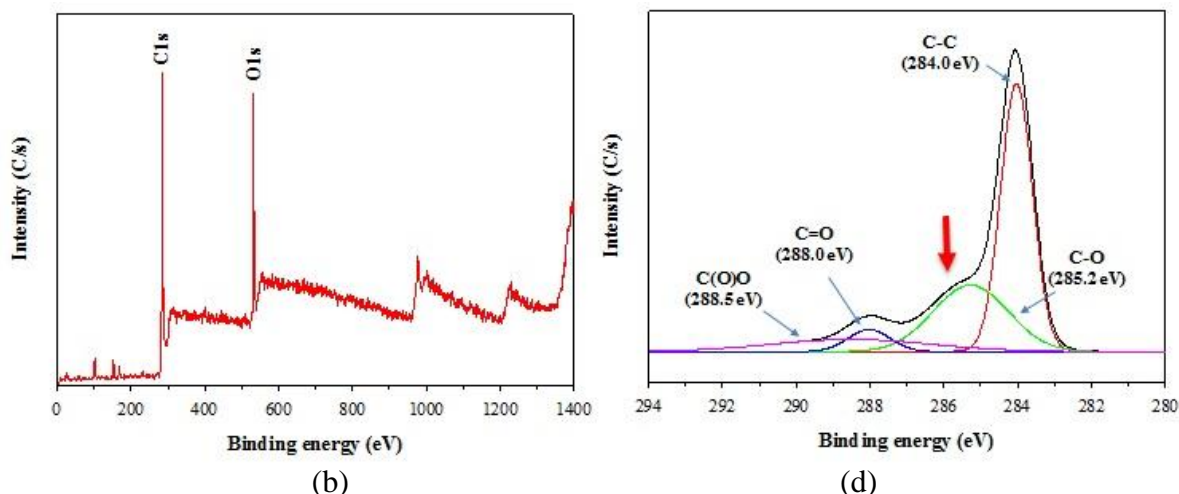


Figure 7. XPS spectra of the GO film (a) before and (b) after UV irradiation for 2 h; C1s XPS spectra (c) before and (d) after UV irradiation for 2h with curve deconvolution.

Figures 7a and b show the XPS spectra of the GO film before and after UV irradiation for 2 h. Strong C1s and O1s peaks were observed in both XPS spectra. The amounts of the C1s and O1s were 71.4 % and 28.6 % before UV irradiation, respectively, and those were 75.7 % and 24.3 % after UV irradiation, respectively. The peak height of C1s before UV irradiation is lower than that of O1s although that after UV irradiation is higher than that of O1s, indicating that oxygen atoms were removed during UV irradiation and the successful UV reduction occurred. The peak deconvolution of the C1s peak can reveal how C atom is connected with O atom as shown in Figures c and d. The main peak at 284 eV was due to the C-C bond. The C-O, C=O, and O=C-O bonds were observed at 285, 288 and 289 eV, respectively. The peak height of the C-O bond decreased a lot after UV irradiation compared to those of the C=O, and O=C-O bonds indicating that the UV reduction mostly occurred through removal of the oxygen atom in C-O bond. The most possible functional groups in GO having C-O bond are hydroxyl and epoxide groups. Thus, the UV reduction might happened mostly at the hydroxyl and epoxide groups in GO.

Preparation of the thin film of the GO/BBL composite on the glass substrate:

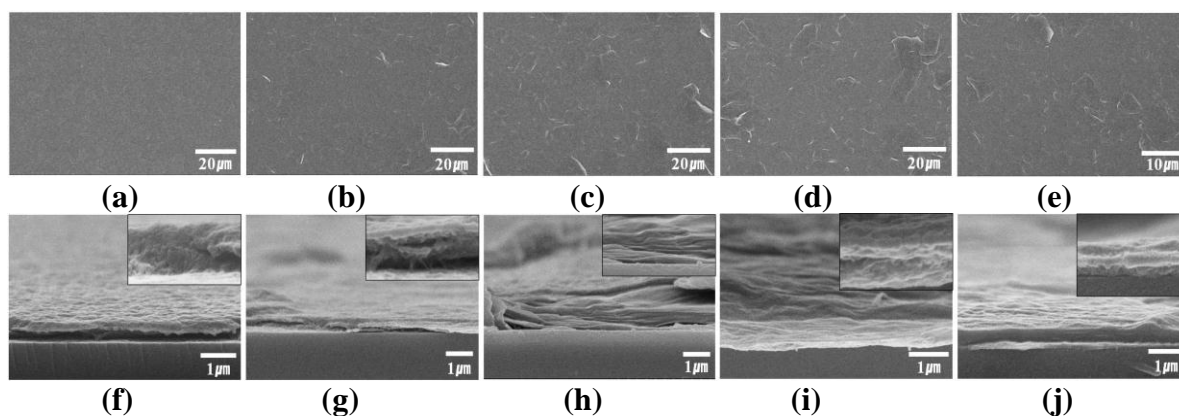


Figure 8. SEM images of the (a, b, c, d, e) top and (f, g, h, i, j) fractured surfaces of the BBL/GO films containing (a, f) 0 (pure BBL), (b, g) 50, (c, h) 60, (d, i) 70, (e, j) 80 wt %

GO.

Figure 8 shows the SEM images of the top and fractured surfaces of the BBL/GO films containing 0 (pure BBL), 50, 60, 60, 80 wt % GO. The top surface of the pure BBL film shows clear image without any protrusion of GO while those of the BBL/GO films do the protrusion of GO. The fractured surfaces of the BBL/GO films show the layered structure inside the film which is more visible as the GO content increases. The layered structure is common in the rigid rod polymers such as poly(p-phenylene benzobisoxazole) (PBO) and poly(p-phenylene benzobisthiazole) (PBT). This layered structure was due to the parallel orientation of the rigid-rod chains along the film surface. The GO might accelerate this parallel orientation due to its plat structure.

UV reduction of the GO/BBL composite film:

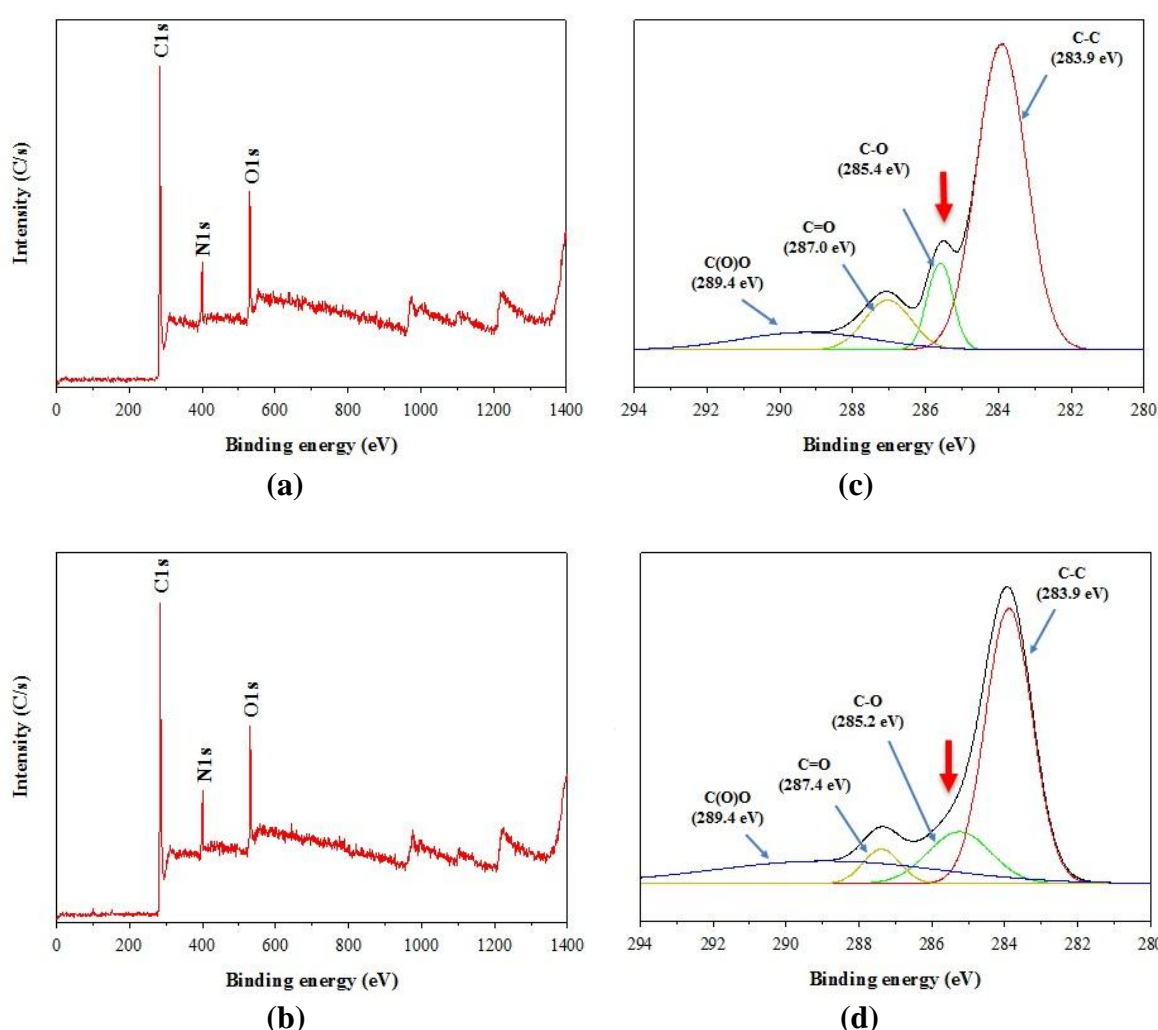
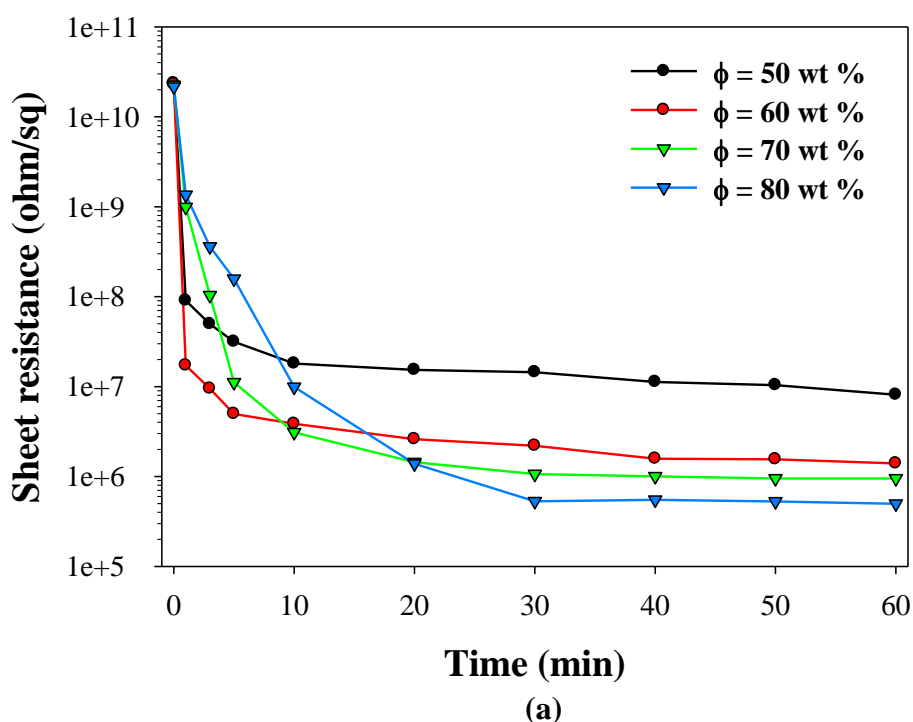


Figure 9. XPS spectra of BBL/GO film ($\phi = 70$ wt %) (a) before and (b) after UV irradiation for 1 h; C1s XPS spectra (c) before and (d) after UV irradiation for 1h.

Figures 9a and b show XPS spectra of the BBL/GO film before and after UV irradiation for 1h. The amounts of the C1s and O1s were 78.5 % and 12.1 % before UV

irradiation, respectively, and those were 78.8 % and 11.6 % after UV irradiation, respectively. The decrease of O1s content compared to C1s was not great. It might be due to a lot of oxygen atoms in BBL which do not participate in reduction process. Figures 9c and d show C1s XPS spectra of the BBL/GO film ($\phi = 70$ wt%) before and after UV irradiation for 1h. The main peak at 283.9 eV was due to the C-C bond. The C-O, C=O, and O=C-O bonds were observed at 285, 288 and 289 eV, respectively. The peak deconvolution showed that the most striking change after UV irradiation was the reduction of the peak height of the C-O band after UV irradiation. The other peaks did not change much after UV irradiation. This result indicates that the hydroxyl and epoxide groups in the GO were removed from the UV irradiation. Thus, we found that the UV reduction of the GO was possible in the BBL/GO composite.



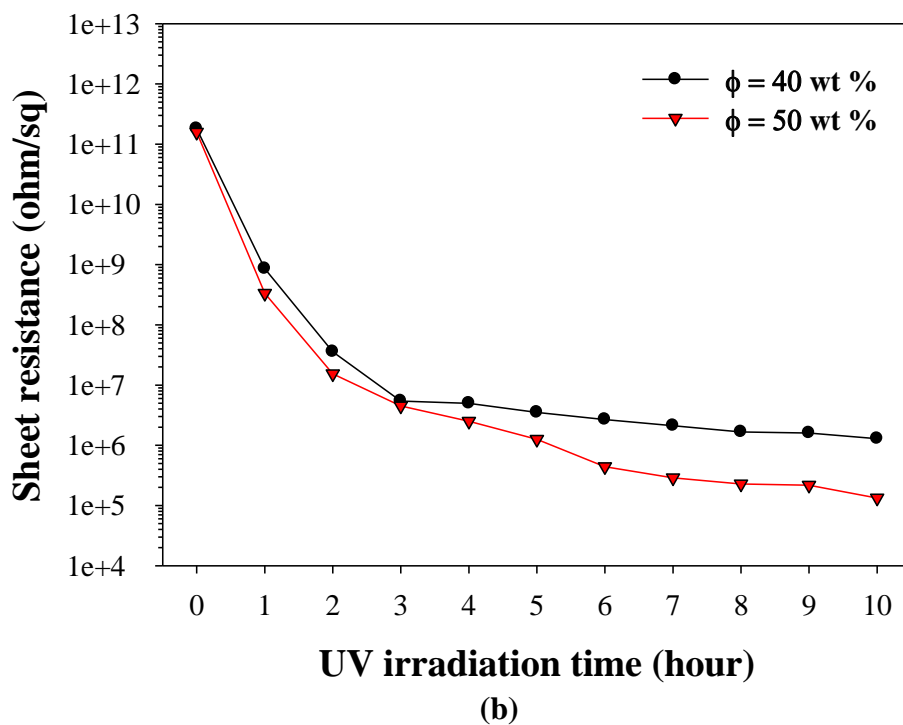


Figure 10. The sheet resistance of (a) BBL/GO ($\phi = 50, 60, 70, 80$ wt%) and (b) PVA/GO ($\phi = 40, 50$ wt%) films as a function of UV irradiation time.

Figure 10 shows the sheet resistance of BBL/GO ($\phi = 50, 60, 70, 80$ wt%) and PVA/GO ($\phi = 40, 50$ wt%) films as a function of UV irradiation time. The sheet resistances of all studied BBL/GO films decreases as UV irradiation time increases, and they are saturated after 30 min (Figure 10a). The sheet resistances of the BBL/GO films before UV irradiation are higher than $10^{10} \Omega/\square$ (almost non-conducting material) and those after UV irradiation for 30 min were 1.4×10^7 , 2.2×10^6 , 1×10^6 , and $5 \times 10^5 \Omega/\square$ for $\phi = 50, 60, 70, 80$ wt%, respectively. Similarly, the sheet resistances of all studied PVA/GO films decreases as UV irradiation time increases, and they are saturated after 3 h (Figure 10b). The sheet resistance of the PVA/GO films before UV irradiation was higher than $10^{10} \Omega/\square$ (almost non-conducting material) and those after UV irradiation for 3 h were 5.41×10^6 , and $4.51 \times 10^6 \Omega/\square$ for $\phi = 40$ and 50 wt%, respectively. As the GO content (ϕ) increases, the final sheet resistance decreases. This is due to the increased amounts of the UV-reducible materials in the composite. Thus, UV irradiation can change the insulating BBL/GO and PVA/GO nanocomposites to conducting materials.

Patterning of PVA/GO nanocomposite:

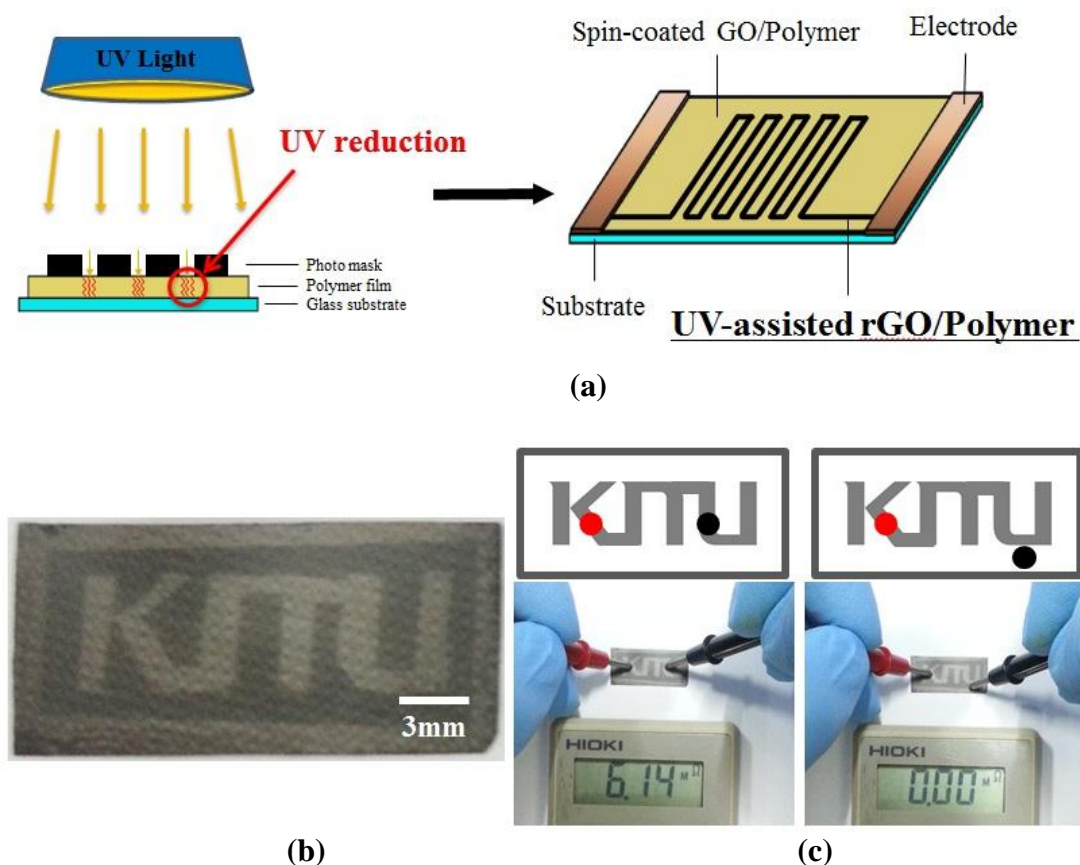


Figure 11. (a) Schematic drawing of UV-assisted patterning on polymer/GO nanocomposite, (b) photographic image of KNU patterned PVA/GO ($\phi = 50$ wt%) film, (c) photographic images showing that the UV-irradiated part is conductive and the UV un-irradiated part is not conductive.

The UV irradiation can be performed on the selective area for patterning as shown in Figure 11a. The appearance of the BBL/GO nanocomposite films after UV patterning were uniform and did not show any patterned shape. It might be due to rigidity of the polymer backbone. In order to demonstrate the UV patterning ability of the polymer/GO composites, the PVA/GO nanocomposite films were prepared and patterned with “KNU” characters as shown in Figure 11b. The clear “KNU” letters were visible. The electrical conductivity was checked with a tester. When the tester probes are on the connected letters, the tester shows the electrical conductivity (Figure 11c). However, when they are the outside of the connected letters, the tester shows no electrical conductivity. This is a demonstration of the UV patterning ability of the GO/polymer composite film although the much more detail studies are necessary for improving the patterning ability to micro or nano meter size.

References:

- ¹ Geim, A. K. **Science** 2009, 324, 1530–1534.
- ² Geim, A. K. **Nat. Mater.** 2007, 6, 183–191.
- ³ Novoselov, K. S. Geim, A. K. Morozov, S. V. Jiang, D. Katsnelson, M. L. Grigorieva, I. V. Dubonos, S. V. Firsov, A. A. **Nature** 2005, 438, 197–200.
- ⁴ Allen, M. J. Tung, V. C. Kaner, R. B. **Chem. Rev.** 2009, 110, 132–145.

- ⁵ Rao, C. N. R. Sood, A. K. Subrahmanyam, K. S. Govindaraj, A. **Angew. Chem. Int. Ed.** 2009, 48, 7752–7777.
- ⁶ Wu, J. Pisula, W. Mullen, K. **Chem. Rev.** 2007, 107, 718–747
- ⁷ Bai, J. Zhong, X. Jiang, S. Huang, Y. Duan, X. **Nat. Nanotechnol.** 2010, 5, 190–194.
- ⁸ Novoselov, K. S. Jiang, Z. Zhang, Y. Morozov, S. V. Stormer., H. L. Zeitler, U. Maan, J. C. Boebinger, G. S. Kim, P. Geim, A. K. **Science** 2007, 315, 1379.
- ⁹ Eda, G. Fanchini, G. Chhowalla, M. **Nat. Nanotechnol.** 2008, 3, 270–274.
- ¹⁰ Kamat, P. V. **J. Phys. Chem. Lett.** 2010, 1, 520–527.
- ¹¹ Seger, B. Kamat, P. V. **J. Phys. Chem. C** 2009, 113, 7990–7995.
- ¹² Li, D. Kaner, R. B. **Science** 2008, 320, 1170–1171.
- ¹³ Hummers, W. S. Offeman, R. E. **J. Am. Chem. Soc.** 1958, 80, 1339–1339.
- ¹⁴ Nakajima, T. Mabuchi, A. Hagiwara, R. **Carbon** 1988, 26, 357–361.
- ¹⁵ Cai, W. W. Piner, R. D. Stadermann, F. J. Park, S. Shaibat, M. A. Ishii, Y. Yang, D. X. Velamakanni, A. An, S. J. Stoller, M. An, J. H. Chen, D. M. Ruoff, R. S. **Science** 2008, 321, 1815–1817.
- ¹⁶ Stankovich, S. Dikin, D. A. Dommett, G. H. B. Kohlhaas, K. M. Zimney, E. J. Stach, E. A. Piner, R. D. Nguyen, S. T. Ruoff, R. S. **Nature** 2006, 442, 282–286.
- ¹⁷ Stankovich, S. Dikin, D. A. Piner, R. D. Kohlhaas, K. A. Kleinhammes, A. Jia, Y. Wu, Y. Nguyen, S. T. Ruoff, R. S. **Carbon** 2007, 45, 1558–1565.
- ¹⁸ Gilje, S. Han, S. Wang, M. Wang, K. L. Kaner, R. B. **Nano Lett.** 2007, 7, 3394–3398.
- ¹⁹ Li, D. Muller, M. B. Gilje, S. Kaner, R. B. Wallace, G. G. **Nat. Nanotechnol.** 2008, 3, 101–105.
- ²⁰ Tung, V. C. Allen, M. J. Yang, Y. Kaner, R. B. **Nat. Nanotechnol.** 2009, 4, 25–29.
- ²¹ Becerril, H. A. Mao, J. Liu, Z. Stoltenberg, R. M. Bao, Z.; Chen, Y. **ACS Nano** 2008, 2, 463–470.
- ²² Schniepp, H. C. Li, J. L. McAllister, M. J. Sai, H. Herrera-Alonso, M. Adamson, D. H. Prud'homme, R. K. Car, R. Saville, D. A. Aksay, I. A. **J. Phys. Chem. B** 2006, 110, 8535–8539.
- ²³ Gomez-Navarro, C. Weitz, R. T. Bittner, A. M. Scolari, M. Mews, A. Burghard, M. Kern, K. **Nano Lett.** 2007, 7, 3499–3503.
- ²⁴ Wang, X. Zhi, L. J. Mullen, K. **Nano Lett.** 2008, 8, 323–327.
- ²⁵ Akhavan O, Abdolahad M, Esfandiar A and Mohatashamifar M **J. Phys. Chem. C** 2010, 114 12955–9
- ²⁶ Akhavan O and Ghaderi E **J. Phys. Chem. C** 2009, 113 20214–20
- ²⁷ Williams G, Seger B and Kamat P V **ACS Nano** 2008 2 1487–91
- ²⁸ Cote L. J. Huang J. **J. Am. Chem. Soc.** 2009, 131, 11027–11032
- ²⁹ Zhang, Y. Guo, L. Wei, S. He, Y. Xia, H. Chen, Q. Sun, H.-B. Xiao, F. S. **Nano Today** 2010, 5, 15–20.
- ³⁰ Abdelsayed V, Moussa S, Hassan H. M. Aluri H. S. Collinson M. M. Samy El-Shall M. **J. Phys. Chem. Lett.** 2010, 1, 2804–2809
- ³¹ Allen M. C. Tung V. C. Gomez L. Xu Z. Chen L. M. Nelson K. S. Zhou C. W. Kaner R. V. Yang Y. **Adv. Mater.** 2009, 21, 2098.

- ³² Chen J.H. Ishigami M. Jang C. Hines D. R. Fuhrer M. S. Williams E. D. **Adv. Mater.** 2007, 19,3623.
- ³³ Liang X. G. Fu Z. L. Chou S.Y. **Nano Lett.** 7, 3840.
- ³⁴ Hendricks T. R. Lu J. Drzal L. T. Lee I. **Adv. Mater.** 2008, 20, 2008.
- ³⁵ Pang S. Tsao H. N. Feng X. Mullen K. **Adv. Mater.** 2009, 21, 1.
- ³⁶ Cote L. J. Cruz-Silva R. Huang J **J. Am. Chem. Soc.** 2009, 131, 11027.
- ³⁷ Kim K. S. Zhao Y. Jang H. Lee S.Y. Kim J. M. Kim K. S. Ahn J.H. Kim P. Choi J.Y. Hong B. H. **Nature** 2009,457,706.
- ³⁸ Berger C. Song Z. M. Li X. B. Wu X. S. Brown N. Naud C. Mayou D. Li T. B. Hass J. Marchenkov A. N. Conrad E. H. De Heer W. A. **Science** 2006, 312, 1191.
- ³⁹ Du D. Liu X. Korn G. Squier J. Mourou G. **Appl. Phys. Lett.** 1994, 64, 3071.
- ⁴⁰ Gattass R. R. Mazur E. **Nature Photon.** 2008, 2, 219.
- ⁴¹ Kawata S. Sun H. B. Tanaka T. Takaba K. **Nature** 2001, 412, 697.
- ⁴² Park J. H. Choudhury A. Farmer B.L. Dang T.D. Park S.Y. **Polymer**, 2012, 53, 3937-3945

List of Publications and Significant Collaborations that resulted from your AOARD supported project:

- Based on these results, a manuscript is being prepared and submitted soon.
- The invited presentation at the Polymer Society of Korea spring meeting 2013 with a title of “**Novel nanocomposites with graphene oxide**”
- The work was discussed with Dr. Loon-Seng Tan at Air Force Research Laboratory (AFRL) and initial BBL was supplied by Dr. Thuy Dang at AFRL.